12. Spielmann, P. E. To what extent did the ancient Egyptians employ bitumen for embalming? *J. Egypt. Archaeol.* **XVIII,** 177–180 (1932).
13. Zaki, A. & Iskander, Z. Materials and methods used for mummifying the body of Amentefnekht, Saqqara 1941. *Ann. Serv. Antiquites Egypte* **XLII,** 223–255 (1943).
14. Rullkötter, J. & Nissenbaum, A. Dead Sea asphalt in Egyptian mummies: molecular evidence. *Naturwissenschaften* **75,** 618–621 (1988).
15. Colombini, M. P., Modugno, F., Silvano, F. & Onor, M. Characterization of the balm of an Egyptian mummy from the seventh century B.C. *Stud. Conserv.* **45,** 19–29 (2000).
16. Koller, J., Baumer U., Kaup Y., Etspüler, H. & Weser, U. Embalming was used in Old Kingdom. *Nature* **391,** 343–344 (1998).
17. Buckley, S. A., Stott, A. W. & Evershed, R. P. Studies of organic residues from ancient Egyptian mummies using high temperature-gas chromatography-mass spectrometry and sequential thermal desorption-gas chromatography-mass spectrometry and pyrolysis-gas chromatography-mass spectrometry. *Analyst* **124,** 443–452 (1999).
18. Mills, J. S. & White, R. *The Organic Chemistry of Museum Objects* 2nd edn (Butterworth-Heinemann, Oxford, 1994).
19. Raven, M. J. Wax in Egyptian magic and symbolism. *Oudheidkundige Mededeelingen uit het Rijksmuseum van Oudheden te Leiden* **64,** 7–47 (1983).
20. van der Doelen, G. A., van den Berg, K. J. & Boon, J. J. Comparative chromatographic and mass spectrometric studies of triterpenoid varnishes: fresh material and aged samples from paintings. *Stud. Conserv.* **43,** 249–264 (1998).
21. Serpico, M. & White, R. in *Ancient Egyptian Materials and Technology* (eds Nicholson, P. T. & Shaw, I.) 430–474 (Cambridge Univ. Press, Cambridge, 2000).
22. Barber, M. S., McConnell, V. S. & DeCaux, B. S. Antimicrobial intermediates of the general phenylpropanoid and lignin specific pathways. *Phytochemistry* **54,** 53–56 (2000).
23. Bahn, P. G. The making of a mummy. *Nature* **356,** 109 (1992).
24. Connan, J. & Dessort, D. Du bitume dans des baumes de momies égyptiennes (1295 av. J.-C. -300 ap. J.-C.): détermination de son origine et evaluation de sa quantité. *C. R. Acad. Sci. Paris II* **312,** 1445–1452 (1991).
25. Granville, A. B. An essay on Egyptian mummies, with observations on the art of embalming amongst the ancient Egyptians. *Phil. Trans. R. Soc. Lond.* **115,** 269–316 (1825).

Acknowledgements

We thank S. Giles of Bristol Museum; J. Spencer and J. Taylor of the British Museum; J. Hayward of Liverpool Museum; R. David of Manchester Museum; and K. Eremin of the National Museum of Scotland for making the samples available to us. We thank J. Fletcher for advice on aspects of Egyptology; and J. Carter and A. Gledhill for technical assistance. NERC provided financial support for mass spectrometry facilities.

Correspondence and requests for materials should be addressed to R.P.E.

Local interactions predict large-scale pattern in empirically derived cellular automata

J. Timothy Wootton

Department of Ecology & Evolution, The University of Chicago, Chicago, Illinois 60637, USA

An important unanswered question in ecology is whether processes such as species interactions that occur at a local scale can generate large-scale patterns seen in nature[1,2]. Because of the complexity of natural ecosystems, developing an adequate theoretical framework to scale up local processes has been challenging. Models of complex systems can produce a wide array of outcomes; therefore, model parameter values must be constrained by empirical information to usefully narrow the range of predicted behaviour. Under some conditions, spatially explicit models of locally interacting objects (for example, cells, sand grains, car drivers, or organisms), variously termed cellular automata[3,4] or interacting particle models[5], can self-organize to develop complex spatial and temporal patterning at larger scales in the absence of any externally imposed pattern[1,6–8]. When these models are based on transition probabilities of moving between ecological states at a local level, relatively complex versions of these models can be linked readily to empirical information on ecosystem dynamics. Here, I show that an empirically derived cellular automaton model of a rocky intertidal mussel bed based on local interactions correctly predicts large-scale spatial patterns observed in nature.

Mussel beds characterize many temperate, rocky intertidal shores throughout the world[9], and can exhibit complex patterning. This patterning is thought to result from the interplay between interactions among sessile species and external disturbance agents, particularly large waves[10–15]. Along the Pacific coast of North America, California mussels (*Mytilus californianus*) seem to interact locally with other organisms in two ways. First, mussels invade bare rock or displace species adjacent to them by overtopping their neighbours as they grow, and by creeping into adjacent areas by means of sequential attachment of new byssal threads in uncolonized areas as old byssal threads in colonized areas break or become detached[12]. Second, because mussels attach to each other with byssal threads, when waves dislodge a mussel from the rock that mussel pulls its neighbours along with it, thereby transmitting the disturbance through the mussel bed in much the same way as forest fires propagate when sparks from a burning tree ignite neighbouring trees[12]. Wave disturbance also acts differentially on mussel beds of different ages, with beds of old, multi-layered mussels being more prone to disturbance, owing to the high ratio of mussel mass per unit attachment area to the rocks, and to the high fraction of byssal threads attached to other mussels, rather than the rock[12,14,15]. Other sessile species and their mobile associates colonize the bare rock created by disturbance events, and exhibit a complex set of interactions among themselves and with mussels[10,12,13,16–19]. Because of its rapid dynamics and macroscopic organisms of modest size and mobility, the rocky intertidal zone is an unusually tractable model system in ecology for experimental investigations and for readily observing spatial and temporal dynamics in a complex natural ecosystem[19]. These features make mussel beds particularly suitable for the purpose of developing and testing different versions of models with empirical parameters, such as cellular automata.

Data on the dynamics of mussel beds were collected over a six-year period (May 1993 to May 1999) at 1,400 fixed points in the mussel bed of Tatoosh Island in Washington State[20]. The data were taken from 14 quadrats (60 × 60 cm) positioned with fixed corner

Figure 1 Photograph of spatial patterning in the mussel bed of Tatoosh Island, Washington.

pins, containing a 10×10 coordinate grid that was defined by monofilament lines spaced 6 cm apart. The ecological state (bare space, species identity, or size class of a species) of each point was determined at both a spring (May) and autumn (late August to early September) census each year. The occurrence or absence of a disturbance event after the previous census was noted for each point. These data were converted into transition probabilities and applied to a cellular automaton model of the mussel bed. The model was based on a 100×300 array of 6×6 cm cells with absorbing boundaries, which is similar in scale (6×18 m) to the average-sized mussel bed on individual rock benches in the intertidal zone of the study site[12]. The full model included 15 ecological states (see Methods), substantially more than many cellular automata[6]. It also incorporated seasonal differences in transition and disturbance rates, and effects of having neighbouring mussels on transition rates (see Methods). The model ran for 500 simulated years, which minimized transient dynamics, and model output was collected on the cumulative average proportion of ecological states and on the distribution of gap sizes. Gap sizes were defined as the number of consecutive steps in random transect lines through the simulated mussel bed taken without encountering a cell filled with a mussel. These model predictions were tested against the size frequency distribution of gaps and the proportional composition of ecological states observed in independent transects taken in the mussel zone of the study site (see Methods).

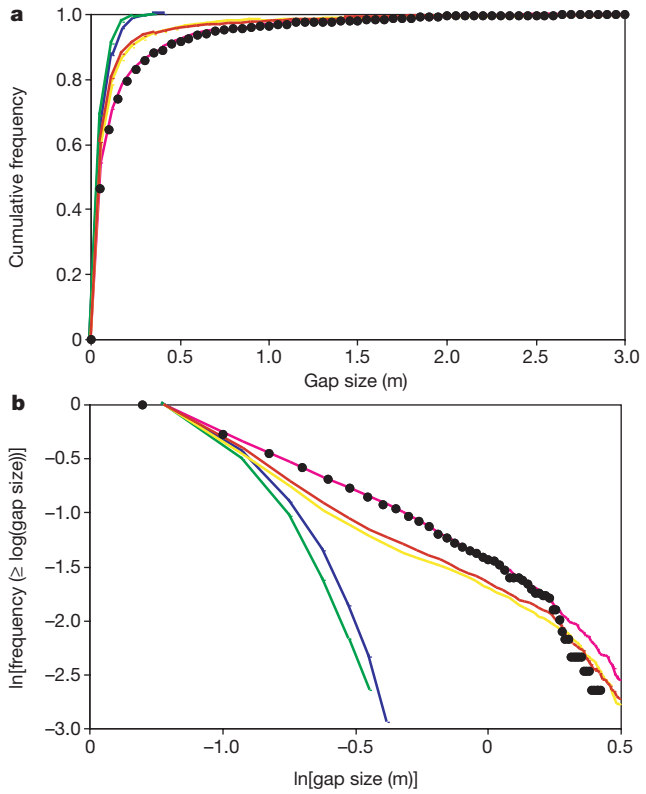

Figure 2 Frequency distribution of gap size (length of consecutive non-*M. californianus* points encountered in random transects) observed in mussel beds of Tatoosh Island, Washington (filled circles; $n = 876$), and generated by various versions of mussel-bed models that had empirical parameters. **a**, Standard cumulative frequency distribution of gap sizes. Pink line, local interactions and disturbance propagation ($P > 0.25$); purple line, non-spatial Markov model ($P < 0.00001$); green line, local interactions only ($P < 0.00001$); yellow line, mussels/no mussels, size structure ($P < 0.0001$); red line, forest fire model, mussel-bed parameters ($P < 0.0001$). **b**, Plot of log-reverse cumulative frequency (log frequency of gaps larger than the gap size in question) versus log gap size. Power law patterns appear as approximately linear curve segments in **b**. Colours are to the same scheme as **a**.

Figure 3 Example of spatial structure generated by the mussel-bed simulation model with external wave-initiated disturbance events. Black points are sites occupied by *M. californianus*. New gaps are dominated by rock (grey) and ephemeral algae (green) points. Older gaps with a variety of algal and invertebrate taxa are represented by different colours (for example: pink, *C. vancouveriensis*; blue, *M. trossulus*; white, *P. polymerus*).

Real mussel beds exhibit strong spatial patterning (Figs 1 and 2; $n = 876$). Results of the full model with empirical parameters self-organized to produce strong spatial patterning (Fig. 3). The distribution of gap sizes from random transects that were generated from the model followed a distribution similar to that observed from real mussel beds (Kolmogorov–Smirnov test, $P > 0.25$; Fig. 2). Additionally, the model accurately predicted the composition of ecological states observed in the study site (Fig. 4; 92.5% of the variance in composition correctly predicted).

Variants of the model were also explored to determine which processes were essential to the results of the model (see Box 1). Features of the full model that were altered included (1) eliminating all spatial structure; (2) removing explicit consideration of all taxa other than *M. californianus*; (3) eliminating the effects of mussel size structure; and (4) altering how disturbance was treated in the model by not explicitly considering the disturbance process. In all cases, the observed distribution of gap sizes differed significantly from model predictions (Kolmogorov–Smirnov tests, all $P < 0.0001$; Fig. 2). Therefore, details of species interactions, size structure, interactions among neighbours and the nature of disturbance impact and propagation were all essential in accurately predicting empirically observed spatial patterning.

In contrast to spatial patterning, the taxonomic composition of the community was accurately predicted by all model variants that included multiple taxa (Fig. 4), including a non-spatial Markov chain model[20], which predicted 98.4% of the variance in taxonomic composition. The high degree of predictive ability in this model suggests either that the observed spatial patterning is not an important determinant of the community composition of sessile

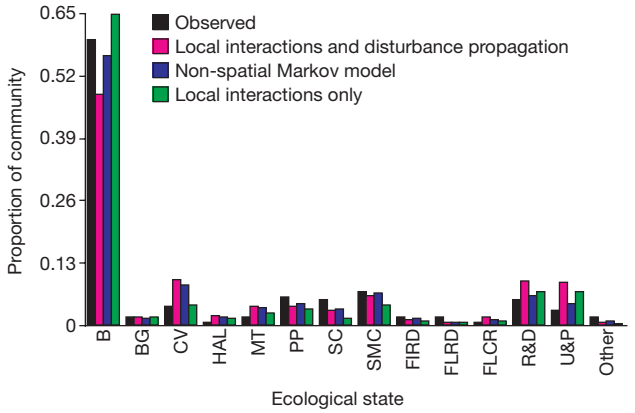

Figure 4 Composition of the mussel-bed community in each ecological state observed from transects (black bars) and predicted by different mussel-bed models with empirical parameters. B, large *M. californianus*; BG, *B. glandula*; CV, *C. vancouveriensis*; HAL, *H. glandiforme*; MT, *M. trossulus*; PP, *P. polymerus*; SC, *S. cariosus*; SMC, small *M. californianus*; FIRD, filamentous red algae; FLRD, foliose red algae; FLCR, fleshy crustose algae; R&D, rock and diatoms; U&P, ephemeral algae; Other, other taxa.

species, or that its effects are adequately subsumed into the parameter estimates of the non-spatial model. Furthermore, this result indicates that developing spatially explicit models that are data intensive may be unnecessary to understand and study compositional aspects of this system.

Model variants that differed in their treatment of disturbance (Box 1) provided some insight into the role of disturbance in pattern formation. A cellular automaton model variant in which transitions depended on neighbours, but which did not explicitly model disturbance, failed to produce patterning (Fig. 2), demonstrating that local interactions alone were insufficient to generate the observed, strong spatial patterning. In contrast, a model variant that lacked size structure and did not account explicitly for other species produced strong spatial patterning, but with a different distribution of gap sizes than was observed (Fig. 2; more small gaps and fewer very large gaps). This model, with parameters estimated from the mussel bed, is identical to the well studied forest fire model[7,21,22], for which self-organized critical behaviour has been reported. Another variant of the full-mussel-bed model that included all features of the full model except for other species generated a gap-size distribution very similar to the distribution of the forest fire model. Therefore, the details of interactions among other species within the community are primarily responsible for the deviations in the pattern of gap size between the full model and the forest fire model.

The results of this study demonstrate that empirically observed rates of species transitions and disturbance can produce self-organized behaviour in a cellular automaton model of the intertidal ecosystem. Furthermore, this self-organized patterning predicts well the patterning seen in nature. The results also indicate that details of size structure and species interactions are important in accurately generating natural patterning. The development of natural patterning only after incorporating external disturbance propagation suggests, however, that conditions in the single-species forest fire models required to generate self-organized patterning, including low disturbance probability and markedly slower rates of recovery relative to disturbance propagation[21], are important characteristics of the system.

A principal unanswered question in ecology is whether interactions at experimentally tractable local scales can be scaled up to recreate larger-scale patterns. Finding approaches that can successfully scale up local processes in complex systems is vital to ensure that detailed mechanistic studies are broadly relevant, and may be essential to fully understanding and predicting the impacts of environmental change[1]. Furthermore, such approaches must be empirically accessible to be applied usefully. Using a cellular automaton framework and transition probabilities derived from a study of small-scale interactions (operating on an aerial scale of 36 cm^2), I successfully reproduced patterning over an area that was more than four orders of magnitude larger. Therefore, it seems possible under some circumstances to derive insight into regional patterns from detailed studies of ecological processes at smaller, tractable scales. □

Box 1

Summary of model variants examined and their essential differences

Full cellular automaton model. This model contained 15 ecological states, which accounted for species/taxonomic composition, empty space and mussel size/age structure. Disturbance was explicitly included by initiating disturbance at randomly assigned points and propagating the disturbance according to empirically observed rates of transmission. Transitions among ecological states were conditional on the season, the presence of mussel neighbours and whether a site was disturbed.

Markov chain model[20]. Transitions among the 15 ecological states were not conditional on spatial arrangement. There was no dependency on neighbours and no explicit modelling of disturbance.

Local interactions model. Transitions among the 15 ecological states were conditional on the presence of neighbouring mussels. There was no explicit modelling of disturbance.

Basic mussel/no mussel model (forest fire model[7,21,22]). For this model there were two ecological states (mussels, no mussels). There were no effects of interactions among other species or effects of mussel size/age class. Disturbance was explicitly modelled as in the full cellular automaton model. There were no seasonal effects.

Detailed mussel/no mussel model. This model included mussel size/age structure, seasonal effects and explicit disturbance as modelled in the full cellular automaton model. There were no effects of interactions among other species.

Methods

Ecological states included in the model

The 15 ecological states included bare space (with and without diatoms); three size/age classes of mussels (<2 cm wide (small mussel); >2 cm wide, newly occupying a site (new, large mussel); >2 cm wide occupying a site for more than one consecutive census (old, large mussel)); and 11 categories representing other common species (*Balanus glandula*, *Corallina vancouveriensis*, *Halosaccion glandiforme*, *Mytilus trossulus*, *Pollicipes polymerus*, *Semibalanus cariosus*) or clumped functional groups (filamentous red algae, foliose red algae, fleshy crustose algae, foliose ephemeral algae and all other taxa)[20]. Rarer species were clumped into functional groups to ensure that sample sizes were sufficiently large to estimate transition probabilities.

Model simulation procedure

First, potential disturbance-initiation events were assigned randomly to single grid cells on the basis of previously reported numbers of disturbance events on rock benches of known area[12], divided by the observed proportion of points in the quadrats occupied by large, old mussels. Second, a disturbance was initiated at any cell to which a disturbance event was assigned if that cell contained an old large mussel. Third, for each newly disturbed cell that had been occupied by an old, large mussel, the model transmitted disturbance to the four nearest neighbours, on the basis of the observed probability that the disturbance was transmitted locally, which was derived from the quadrat data. The third step was repeated until no new disturbed cells were generated. Finally, transitions were randomly assigned to each cell on the basis of empirically derived transition probabilities that depended on the prior species identity of the cell, whether the cell was disturbed, and whether the cell previously had at least one mussel as a neighbour. The entire procedure was repeated alternately for parameters derived for summer (May–September) and winter (September–May).

Derivation of empirically observed patterns to test model

Observed composition and gap-size data were collected from transects that were randomly placed through the mussel bed at various spots throughout the study site. For composition measures, the ecological state under points at 0.5 m intervals were recorded (n = 1,128)[20]. In a second series of transects measuring gap sizes, the presence or absence of mussels was noted at 5-cm intervals and gap size was defined as the number of sequential observations of points without mussels (n = 876 gaps). These data were tested against model predictions, which were best-fit functions for the cumulative gap size distributions generated by the model using nonlinear least squares regression. The best-fit functions were compared with the observed cumulative gap-size distribution using one-sample Kolmogorov–Smirnov tests[23].

Received 5 July; accepted 6 September 2001.

1. Levin, S. A. The problem of pattern and scale in ecology. *Ecology* **73,** 1943–1967 (1992).
2. Wiens, J. A., Stenseth, N. C., Van Horne, B. & Ims, R. A. Ecological mechanisms and landscape ecology. *Oikos* **66,** 369–380 (1993).
3. Wolfram, S. Cellular automata as models of complexity. *Nature* **311,** 419–424 (1984).
4. Ermentrout, G. B. & Edelstein-Keshet, L. Cellular automata approaches to biological modeling. *J. Theor. Biol.* **160,** 97–133 (1993).
5. Durrett, R. & Levin, S. A. Stochastic spatial models: a user's guide to ecological applications. *Phil. Trans. R. Soc. Lond. B* **343,** 329–350 (1994).
6. Bak, P. *How Nature Works: The Science of Self-organized Criticality* (Copernicus, New York, 1996).
7. Jensen, J. H. *Self-organized Criticality* (Cambridge Univ. Press, Cambridge, 1998).
8. Solé, R. V. & Manrubia, S. C. Are rainforests self-organized in a critical state? *J. Theor. Biol.* **173,** 31–40 (1995).
9. Stephenson, T. A. & Stephenson, A. *Life between Tidemarks on Rocky Shores* (Freeman, San Francisco, 1972).

10. Dayton, P. K. Competition, disturbance, and community organization: the provision and subsequent utilization of space in a rocky intertidal community. *Ecol. Monogr.* **41,** 351–389 (1971).
11. Levin, S. A. & Paine, R. T. Disturbance, patch formation, and community structure. *Proc. Natl Acad. Sci. USA* **71,** 2744–2747 (1974).
12. Paine, R. T. & Levin, S. A. Intertidal landscapes: disturbance and the dynamics of pattern. *Ecol. Monogr.* **51,** 145–178 (1981).
13. Sousa, W. P. Intertidal mosaics: patch size, propagule availability and spatially variable patterns of succession. *Ecology* **65,** 1918–1935 (1984).
14. Denny, M. W. Lift as a mechanism of patch initiation in mussel beds. *J. Exp. Mar. Biol. Ecol.* **113,** 231–246 (1987).
15. Wootton, J. T. Size-dependent competition: effects on the dynamics vs. the end point of mussel bed succession. *Ecology* **74,** 195–206 (1993).
16. Johnson, L. E. Potential and peril of field experimentation: the use of copper to manipulate molluscan herbivores. *J. Exp. Mar. Biol. Ecol.* **160,** 251–262 (1992).
17. Wootton, J. T. Indirect effects, prey susceptibility, and habitat selection: impacts of birds on limpets and algae. *Ecology* **73,** 981–991 (1992).
18. Wootton, J. T. Predicting direct and indirect effects: an integrated approach using experiments and path analysis. *Ecology* **75,** 151–165 (1994).
19. Paine, R. T. *Marine Rocky Shores and Community Ecology: An Experimentalist's Perspective* (Ecology Institute, Olendorf, Germany, 1994).
20. Wootton, J. T. Prediction in complex communities: analysis of empirically-derived Markov models. *Ecology* **82,** 580–598 (2001).
21. Clar, S., Drossel, B. & Schwabl, F. Forest fires and other examples of self-organized criticality. *J. Phys. Condens. Matter* **8,** 6803–6824 (1996).
22. Malamud, B. D., Morein, G. & Turcotte, D. L. Forest fires: an example of self-organized critical behavior. *Science* **281,** 1840–1842 (1998).
23. Sokal, R. R. & Rohlf, F. J. *Biometry* (Freeman, New York, 1995).

Acknowledgements

I thank the Makah Tribal Council and the United States Coast Guard for providing access to Tatoosh Island; A. Miller, R. Raynor, K. Rose, J. Salamunovitch, B. Scott, J. Sheridan, F. Stevens and A. Sun for field assistance; and P. Kareiva, R. Paine, C. Pfister and A. Sun for helpful comments. The work was supported in part by the A. W. Mellon Foundation and personal funds.

Correspondence and request for materials should be addressed to J.T.W. (e-mail: twootton@uchicago.edu).

Perceptual learning without perception

Takeo Watanabe*, José E. Náñez† & Yuka Sasaki‡

** Department of Psychology, Boston University, 64 Cummington Street, Boston, Massachusetts 02215, USA*
† Department of Social and Behavioral Sciences, Arizona State University West, Phoenix, Arizona 85069-7100, USA
‡ NMR Center, Massachusetts General Hospital, Charlestown, Massachusetts 02129, USA

The brain is able to adapt rapidly and continually to the surrounding environment, becoming increasingly sensitive to important and frequently encountered stimuli[1–4]. It is often claimed that this adaptive learning is highly task-specific, that is, we become more sensitive to the critical signals in the tasks we attend to[5–15]. Here, we show a new type of perceptual learning, which occurs without attention, without awareness and without any task relevance. Subjects were repeatedly presented with a background motion signal so weak that its direction was not visible; the invisible motion was an irrelevant background to the central task that engaged the subject's attention. Despite being below the threshold of visibility and being irrelevant to the central task, the repetitive exposure improved performance specifically for the direction of the exposed motion when tested in a subsequent suprathreshold test. These results suggest that a frequently presented feature sensitizes the visual system merely owing to its frequency, not its relevance or salience.

We repeatedly presented a dynamic random dot (DRD) display[16] with a small number of temporarily, coherently moving (signal) dots and a much larger number of randomly moving (noise) dots in the background. During this display, subjects conducted an identification task of letters that were presented at the centre of the display[17] so that motion was an irrelevant feature. The ratio of signal to noise dots was a constant 5% during exposure. This signal strength was below the thresholds on tests of direction identification, direction discrimination and coherent motion detection tasks, which were conducted before, during and after the exposure. This suggests that attention and awareness had no access to the motion signal during the letter identification task. Nevertheless, after repeated exposure to this 'invisible', 5% level of coherent motion in the background, a significant performance improvement was obtained only for the motion directions within a small range around the exposed coherent direction when tested with a DRD display with 10% coherent motion. That is, this subsequent test revealed perceptual learning as a result of mere exposure to an 'invisible' motion direction.

The first experiment consisted of an exposure stage that was preceded and followed by control test stages (Fig. 1a). In each trial of

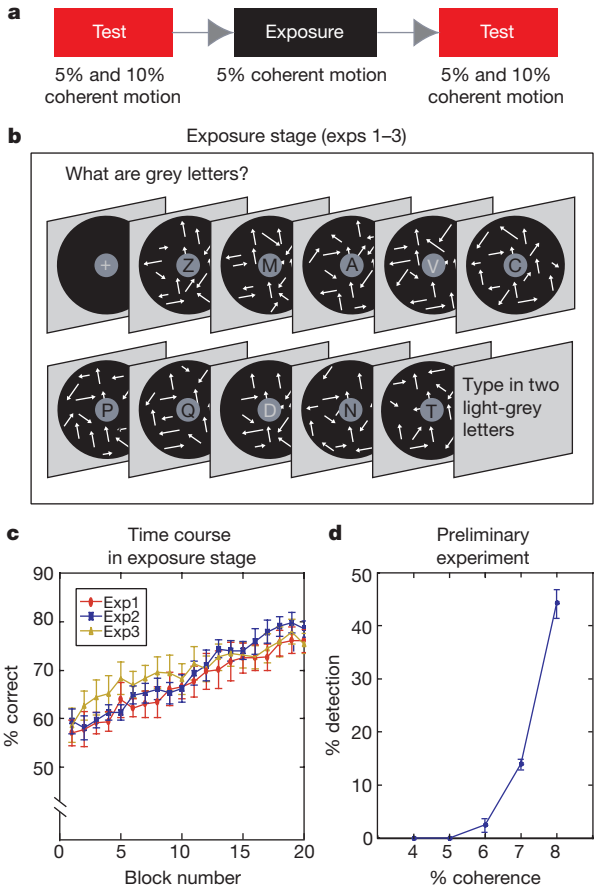

Figure 1 General procedure and exposure stage. **a**, In the exposure stage, dynamic random dot (DRD) displays with 5% coherent motion were presented; these were irrelevant to the task. In the test stages, DRD displays with 5% and 10% coherence were presented; these were relevant to the task. **b**, Exposure stage procedure. A sequence consisted of 8 black letters (0.5 cd m^{-2}) and 2 light-grey letters (53.0 cd m^{-2}) on a 1° diameter, dark-grey circle (32.0 cd m^{-2}), which was within the 10° diameter, black circular background (0.5 cd m^{-2}). Each letter was presented for 33 ms and was followed by a 17-ms blank interval. Thus, the duration of the sequence and the motion background was 500 ms. **c**, Time course of the mean 'correct' percentage (± s.e.) for eight subjects in the exposure stage in experiments 1–3. **d**, Mean percentage (± s.e. for eight subjects) of coherence detection as a function of coherence percentage in the preliminary experiment.